

## Probabilistic strain-fatigue life performance based on stochastic analysis of structural and WAAM-stainless steels

Xin, Haohui; Correia, José A.F.O.; Veljkovic, Milan; Zhang, Youyou; Berto, Filippo; de Jesus, Abílio M.P.

**DOI**

[10.1016/j.engfailanal.2021.105495](https://doi.org/10.1016/j.engfailanal.2021.105495)

**Publication date**

2021

**Document Version**

Final published version

**Published in**

Engineering Failure Analysis

**Citation (APA)**

Xin, H., Correia, J. A. F. O., Veljkovic, M., Zhang, Y., Berto, F., & de Jesus, A. M. P. (2021). Probabilistic strain-fatigue life performance based on stochastic analysis of structural and WAAM-stainless steels. *Engineering Failure Analysis*, 127, 1-20. Article 105495. <https://doi.org/10.1016/j.engfailanal.2021.105495>

**Important note**

To cite this publication, please use the final published version (if applicable). Please check the document version above.

**Copyright**

Other than for strictly personal use, it is not permitted to download, forward or distribute the text or part of it, without the consent of the author(s) and/or copyright holder(s), unless the work is under an open content license such as Creative Commons.

**Takedown policy**

Please contact us and provide details if you believe this document breaches copyrights. We will remove access to the work immediately and investigate your claim.

***Green Open Access added to TU Delft Institutional Repository***

***'You share, we take care!' - Taverne project***

**<https://www.openaccess.nl/en/you-share-we-take-care>**

Otherwise as indicated in the copyright section: the publisher is the copyright holder of this work and the author uses the Dutch legislation to make this work public.



ELSEVIER

Contents lists available at ScienceDirect

# Engineering Failure Analysis

journal homepage: [www.elsevier.com/locate/engfailanal](http://www.elsevier.com/locate/engfailanal)

## Probabilistic strain-fatigue life performance based on stochastic analysis of structural and WAAM-stainless steels

Haohui Xin<sup>a,b</sup>, José A.F.O. Correia<sup>b,c,\*</sup>, Milan Veljkovic<sup>b</sup>, Youyou Zhang<sup>a,\*</sup>,  
Filippo Berto<sup>d</sup>, Abílio M.P. de Jesus<sup>c</sup>

<sup>a</sup> Department of Civil Engineering, School of Human Settlements and Civil Engineering, Xi'an Jiaotong University, China

<sup>b</sup> Faculty of Civil Engineering and Geosciences, Delft University of Technology, Netherlands

<sup>c</sup> INEGI & CONSTRUCT, Faculty of Engineering, University of Porto, Portugal

<sup>d</sup> Department of Mechanical and Industrial Engineering, Norwegian University of Science and Technology (NTNU), Norway

### ARTICLE INFO

#### Keywords:

Coffin-Manson and Morrow's (CMM) equation  
Probabilistic fatigue behaviour  
Latin hypercube sampling strategy  
Structural steels  
Wire arc additive manufacturing (WAAM)  
stainless steel

### ABSTRACT

Wire arc additive manufacturing (WAAM) has increasingly attracted attention in the construction sector because of its ability to produce large metallic structural parts in short times. In this paper, Coffin-Manson and Morrow (CMM) equation is employed to compare the fatigue life of WAAM stainless steel with the structural steels S355 and S690. The results showed that the fatigue performance of structural steel is better than the WAAM stainless steel, the fatigue performance vertical to printing direction (WAAM-900) is better than it along the printing direction (WAAM-00). In addition, the fatigue cycle of the transition reversals of structural steel is much less than it of WAAM stainless. With the increasing the fatigue cycle, the maximum density of the strain amplitude ratio is gradually increased to 1.0. The probabilistic parameters of CMM equation were obtained by a stochastic analysis using Latin hypercube sampling strategies. The probabilistic strain-fatigue life behaviour obtained from the constant exponent sampling strategy is higher when compared with the varied exponent sampling strategy for both WAAM stainless and structural steels.

### 1. Introduction

Additive manufacturing (AM), also referred to as 3D printing, is a technology that forms three-dimensional objects by placing successive layers of raw materials. AM is starting to be used in the infrastructure sector [1–4] attributing to its rapid prototyping advantages. In recent years, wire arc additive manufacturing (WAAM) [5–7], a wire-based directed energy deposition (DED) approach where an electric arc as the heat source and a solid wire as the feedstock material, has increasingly attracted attention in the infrastructural sector. Although the precision of the WAAM as-built parts may be lower than those obtained using powder-bed systems. WAAM is currently being proposed in the construction of civil steel structures by both academia and industry [5–7] by the following reasons: - It is capable to produce large metallic structural parts in short times attributed to high deposition rates; and, - WAAM is much cheaper due to the use of standard off-the-shelf equipment, mature technology, and low material costs.

The fatigue resistance is one of the most important concerns for the application of WAAM steel structures. Fatigue could be

\* Corresponding authors at: Faculty of Civil Engineering and Geosciences, Delft University of Technology, Netherlands (José A.F.O. Correia).

E-mail addresses: [xinhaohui@mail.xjtu.edu.cn](mailto:xinhaohui@mail.xjtu.edu.cn) (H. Xin), [jacorreia@fe.up.pt](mailto:jacorreia@fe.up.pt) (J.A.F.O. Correia), [M.Veljkovic@tudelft.nl](mailto:M.Veljkovic@tudelft.nl) (M. Veljkovic), [zhang\\_0522yy@163.com](mailto:zhang_0522yy@163.com) (Y. Zhang), [filippo.berto@ntnu.no](mailto:filippo.berto@ntnu.no) (F. Berto), [ajesus@fe.up.pt](mailto:ajesus@fe.up.pt) (A.M.P. de Jesus).

<https://doi.org/10.1016/j.engfailanal.2021.105495>

Received 28 February 2021; Received in revised form 21 April 2021; Accepted 6 May 2021

Available online 19 May 2021

1350-6307/© 2021 Elsevier Ltd. All rights reserved.

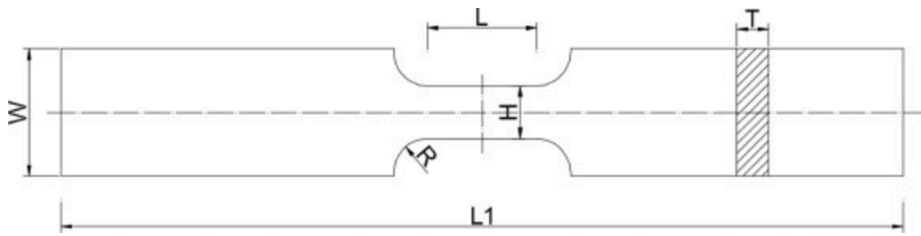


Fig. 1. Geometry of Fatigue Specimens [48].

regarded as damage caused by the changes of microstructure leading to fatigue crack initiation followed by fatigue crack propagation under the time-dependent cyclic loading [8–11]. In terms of fatigue behavior of WAAM steels, Gordon et al. [12] investigated the fatigue crack growth rate of stainless steel alloy 304L fabricated using wire and arc additive manufacturing. The results showed that the fatigue crack growth rate of horizontal and vertical directions is different attributing to long columnar grains and strong texture in the build direction and retained compressive residual stresses. The S-N curves of WAAM stainless steel are also experimentally investigated by uniaxial tension-tension fatigue experiments of specimens parallel and perpendicular to the build direction by Gordon et al. [13]. Wächter et al. [14] investigated the monotonic and cyclic properties of WAAM steels. The results showed that the monotonic properties of WAAM steel are different from the same weld filler material in conventional welding, and the cyclic properties are in good agreement with cast steel. Biswal et al. [15] investigated the effect of internal porosity on the fatigue strength of WAAM titanium alloy, a modified Kitagawa-Takahashi diagram was proposed to predict the fatigue limit, and the critical pore diameter was found to be about 100  $\mu\text{m}$ . Ermakova et al. [16] performed an experimental investigation on the mechanical and fracture properties of WAAM components made of ER70S-6 and ER100S-1 metal wires. The results show that the material hardness and yield strength of the ER100S-1 built wall is higher than ER70S-6 by 62% and 42%, respectively. The results also showed that the yield and ultimate tensile strength values were found to be slightly higher in specimens extracted in deposition direction when compared to specimens extracted in the built direction. J Galan Argumedo [17] investigated the fatigue behavior and mechanical characterization of austenitic stainless-steel components produced through WAAM. The results showed that average fatigue performance is indistinguishable from the mean design values proposed for the structural stainless steels under standardized testing conditions. The material performance is superior to the design curves proposed by ASME.

Current explore of WAAM steel applications in the infrastructure sector includes both modest-scale components and full size structures [1], including pedestrian bridge [18,19], hook [20,21], local stiffener of I-shaped girder [20,21], clamping element [20,21], optimized T-stub endplate [20,21], joints to connect four members [20,21]. The main application of WAAM steels is the replacement or the combination of conventional steel structures. Hence, one of the rising questions is that how much difference in fatigue performance between WAAM steels and traditional structural steels. The fatigue performance differences will affect the design of WAAM steel structures.

In addition, with the increasing attention on structural reliability and integrity, probabilistic fatigue models are generally used to consider the multiple uncertainty sources on fatigue lifetime. Correia [22,23] proposed a probabilistic S-N field based on Castillo & Fernández-Canteli (CFC) model using the Weibull distribution function and UniGrow approach for the notched details. Additionally, Correia [24,25] also suggested a unified fatigue methodology based on a probabilistic Castillo & Fernández-Canteli (CFC) model combined with the strain energy density approach proposed by Huffman [25] applied to structural details. De Jesus [26] presented a study of fatigue strength modelling based on local approach and probabilistic CFC model for riveted connections. Other studies [27–31] on the fatigue strength modeling of materials and structural connections were made based on a linear regression analysis combined with the application of probabilistic distribution functions - Normal, Weibull, etc. Reliable Wöhler curves based on the Stüssi model and the Weibull distribution function were suggested by Caiza et al. [32] to strengthen modelling of structural details. Correia [33] generalized the probabilistic CFC model for various local fatigue damage parameters. Recently, Barbosa [34] presented a review on probabilistic fatigue models applied to metals and composites. Mourão et al. [35] presented a scientific work on the evaluation of fatigue damage of offshore tubular joints using the strain fatigue damage criterion estimated through a probability distribution function. Zhu et al. [36] investigated the fatigue life distribution of notched specimens based on the Weibull model and critical distance theory. It is important to compare the probabilistic fatigue behavior of WAAM steels with structural steels, such as S355 and S690, to provide an initial impression for the designer during replacing traditional structural steel with WAAM plates. Besides, the fatigue crack growth rates (FCGR) modelling based on the J-integral [37], stress intensity factor [38], equivalent initial flaw size (EIFS) [39], and energy-based  $\Delta S^*$  crack driving force [40] approaches, and considering some factors such as the crack closure effects [41], variable amplitude loading [42], and mixed-mode loading conditions [38], can also be supported by probabilistic analysis, as suggested in some researches [10,22,23,24,43,44].

In this paper, Coffin-Manson and Morrow's (CMM) Fatigue equation [45–47] is employed to describe the fatigue life of WAAM stainless steel, structural steels S355 and S690 in the literature [17,48]. The parameters with 95%, 97.7%, and 99% guarantee of CMM Fatigue equation were obtained by a stochastic analysis using Latin hypercube sampling strategies. The exponent effects on the probabilistic parameters of the CMM fatigue equation are investigated by parametric analysis.

**Table 1**

Nominal geometry of specimens [17,48] (Unit: mm).

Materials	W	T	L	L1	H	R
WAAM	20.0	4.0	14.0	200.0	10.0	10.0
S355	30.0	7.5	26.0	200.0	12.5	8.0
S690	16.0	4.0	13.0	110.0	8.0	4.5

**Table 2**

Fatigue test results of WAAM stainless steel along printing direction (0°) [17].

Number	Total Strain Amplitude	Elastic Strain Amplitude	Plastic Strain Amplitude	Stress Range	Fatigue Life
1	0.0117	0.004	0.0077	718.4	867
2	0.0092	0.0028	0.0064	825.4	178
3	0.0092	0.0032	0.0060	642.2	2186
4	0.0072	0.0027	0.0045	637.6	1899
5	0.0072	0.0020	0.0052	572.2	1743
6	0.0056	0.0018	0.0038	521.0	9790
7	0.0056	0.0018	0.0038	509.6	9065
8	0.0044	0.0018	0.0026	533.2	8373
9	0.0034	0.0017	0.0017	502.6	42,909
10	0.0027	0.0018	0.0009	465.4	120,189
11	0.0021	0.0015	0.0006	442.6	904,486
12	0.0021	0.0013	0.0008	379.4	861,736
13	0.0020	0.0017	0.0003	436.8	565,894
14	0.0019	0.0013	0.0006	285.4	2.00E+06 (Run out)
15	0.0019	0.0015	0.0004	380.8	33,869
16	0.0018	0.0015	0.0003	367.8	500,507
17	0.0018	0.0012	0.0006	378.6	869,485
18	0.0017	0.0012	0.0005	345.2	2.00E+06 (Run out)

**Table 3**

Fatigue test results of WAAM stainless steel vertical to printing direction (90°) [17].

Number	Total Strain Amplitude	Elastic Strain Amplitude	Plastic Strain Amplitude	Stress Range	Fatigue Life
1	0.0150	0.0034	0.0116	734.2	879
2	0.0150	0.0042	0.0108	757.0	813
3	0.0117	0.0033	0.0084	759.2	273
4	0.0117	0.0022	0.0095	522.0	8096
5	0.0092	0.0030	0.0062	669.0	3277
6	0.0072	0.0022	0.0050	522.0	8096
7	0.0056	0.0026	0.0030	509.2	19,186
8	0.0044	0.0024	0.0020	584.6	20,352
9	0.0044	0.0022	0.0022	521.6	46,910
10	0.0034	0.0020	0.0014	540.2	34,565
11	0.0034	0.0018	0.0016	502.8	35,920
12	0.0027	0.0020	0.0007	471.0	148,290
13	0.0020	0.0014	0.0006	401.0	1,208,800
14	0.0020	0.0016	0.0004	427.6	283,033
15	0.0019	0.0016	0.0003	387.4	511,028
16	0.0019	0.0014	0.0005	376.8	2.00E+06 (Run out)
17	0.0019	0.0012	0.0007	317.6	2.00E+06 (Run out)
18	0.0018	0.0010	0.0008	396.0	1,637,000
19	0.0017	0.0012	0.0005	346.0	2.00E+06 (Run out)
20	0.0012	0.0009	0.0003	258.0	2.00E+06 (Run out)

## 2. Materials and experimental results

The fatigue behavior of WAAM stainless steel in the literature [17] and structural steel S355/S690 in the literature [48] are compared in this section. In Fig. 1 and Table 1, the configuration of the fatigue specimens and the nominal geometry of these specimens are presented, respectively. In terms of 3D printed steel materials, test coupons are extracted from heat-treated WAAM single-bead walls on the S355 parent plates, fabricated by a six-axis articulated welding robot using SAE316L as the filler materials. The monotonic static properties were tested based on the recommendations of testing standard ASTM E606-606M [49]. The average elastic modulus is 104.1GPa and 111.2GPa, and the average 0.2% yield strength is 347.2 MPa and 321.3 MPa, average tensile ultimate strength is 583.6 MPa and 564.9 MPa for WAAM stainless steel with 0° (longitudinal to the printing direction) and 90° (vertical to the printing direction) direction respectively. More details, such as chemical characterization, X-Ray Diffraction for phase identification

**Table 4**  
Fatigue test results of Structural Steel S355 [48].

Number	Total Strain Amplitude	Elastic Strain Amplitude	Plastic Strain Amplitude	Stress Range	Fatigue Life
1	0.01000	0.00429	0.00571	817.4	4805
2	0.00500	0.00281	0.00219	569.5	16,175
3	0.02000	0.00557	0.01443	975.5	336
4	0.00400	0.00307	0.00093	615.4	29,501
5	0.00300	0.00279	0.00021	536.3	861,304
6	0.00350	0.00299	0.00051	581.5	278,243
7	0.00300	0.00297	0.00003	646.6	191,940
8	0.00400	0.00328	0.00072	661.2	64,244
9	0.02000	0.00573	0.01427	968.2	542
10	0.01000	0.00429	0.00571	817.4	4805

**Table 5**  
Fatigue test results of Structural Steel S690 [48].

Number	Total Strain Amplitude	Elastic Strain Amplitude	Plastic Strain Amplitude	Stress Range	Fatigue Life
1	0.02000	0.00800	0.01200	1555.2	190
2	0.01000	0.00707	0.00293	1401.9	1272
3	0.00500	0.00484	0.00016	1105.0	60,505
4	0.00500	0.00490	0.00010	1062.7	44,819
5	0.01000	0.00692	0.00308	1435.7	1920
6	0.02000	0.00807	0.01193	1590.6	160
7	0.00400	0.00399	0.00001	867.4	131,000
8	0.00400	0.00396	0.00004	879.3	371,000
9	0.00380	0.00379	0.00001	835.6	1,545,579
10	0.01500	0.00739	0.00761	1565.3	410

**Table 6**  
Fitted parameters of CMM equation.

Materials	E (GPa)	$\sigma_f$ (Mpa)		b		$\dot{\epsilon}_f$		c		
		Ave	Std	Ave	Std	Ave	Std	Ave	Std	
WAAM	0°	104.25	272.0	51.5	-0.0924	0.0094	0.0442	0.0191	-0.3644	0.0509
	90°	111.20	438.2	52.7	-0.1168	0.0115	0.1175	0.0505	-0.4292	0.0503
S355		210.50	774.0	105.8	-0.0754	0.0134	0.7134	0.5389	-0.6614	0.1280
S690		209.40	1278.1	161.1	-0.0773	0.0058	0.8062	0.4308	-0.8202	0.0735

and quantification, microscopy for qualitative sub-grain and grain microstructural characterization, stress-strain relationship, etc., can be found in ref. [17]. In terms of structural steel S355 and S690, the steel grades are specified according to the EN10025 standard [50]. Quasi-static monotonic tensile tests were also performed to investigate the basic behavior of S355 and S690. The average value of elastic modulus is 210.5GPa and 209.4GPa, the average 0.2% yield strength is 419.0 MPa and 765.7 MPa, and the average ultimate strength is 732.0 MPa and 823.0 MPa for steel grade S355 and S690, respectively.

Tables 2 and 3 list fatigue test results of WAAM SAE316L stainless steel along and vertical to the printing direction respectively, reported in the reference [17], Table 4 presented fatigue test results of structural steel with the grades S355 according to the reference [48], and Table 5 reported the fatigue test results of S690 based on the literature [48]. The results include the total strain amplitude,  $\Delta\epsilon$ , the elastic strain amplitude,  $\Delta\epsilon_E$ , the plastic strain amplitude,  $\Delta\epsilon_P$ , the stress range,  $\Delta\sigma$ , and the fatigue life,  $N_f$ . The stress ratio for both WAAM stainless and structural steel is -1.0. The Coffin–Manson–Morrow (CMM) equation [45–47], expressed in Eq.(1), is employed to describe the relationship between total strain amplitude and fatigue life. Table 6 summarized the parameters of the CMM relationship for 3D printed stainless steel along the printing direction (WAAM-0°), vertical to the printing direction (WAAM-90°), S355, and S690. Fig. 2 presented a comparison between CMM and experimental results. A good agreement is observed.

$$\frac{\Delta\epsilon}{2} = \frac{\Delta\epsilon_E}{2} + \frac{\Delta\epsilon_P}{2} = \frac{\dot{\sigma}_f}{E}(2N_f)^b + \dot{\epsilon}_f(2N_f)^c \tag{1}$$

where:  $\dot{\sigma}_f$ , b,  $\dot{\epsilon}_f$  and c are materials parameters of the Coffin–Manson–Morrow (CMM) equation.

The comparison of strain-fatigue life relationship between WAAM stainless steel and structural steel is illustrated in Fig. 3. The

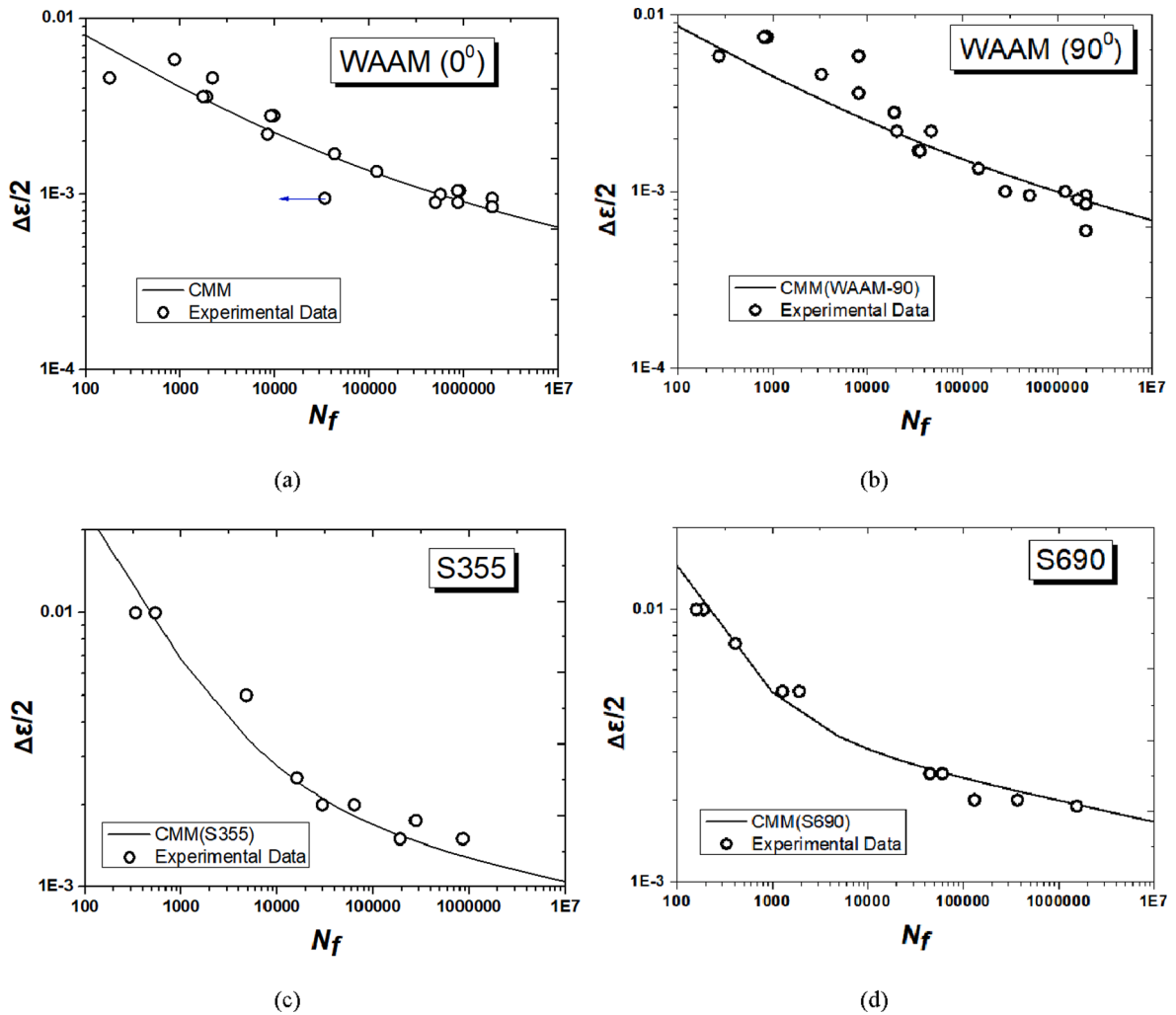


Fig. 2. Comparisons between CMM equation and experimental results.

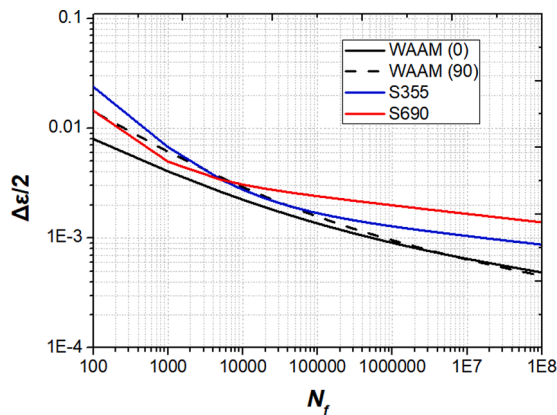


Fig. 3. Fatigue life comparisons between WAAM and Structural Steel.

results showed that the fatigue performance of structural steel is better than the WAAM stainless steel, this is because the elastic modulus of WAAM stainless is lower. The elastic modulus of WAAM stainless steel reported in ref. [17] is almost half of structural steel. In addition, the fatigue performance vertical to the printing direction (WAAM-90°) is better than it along the printing direction

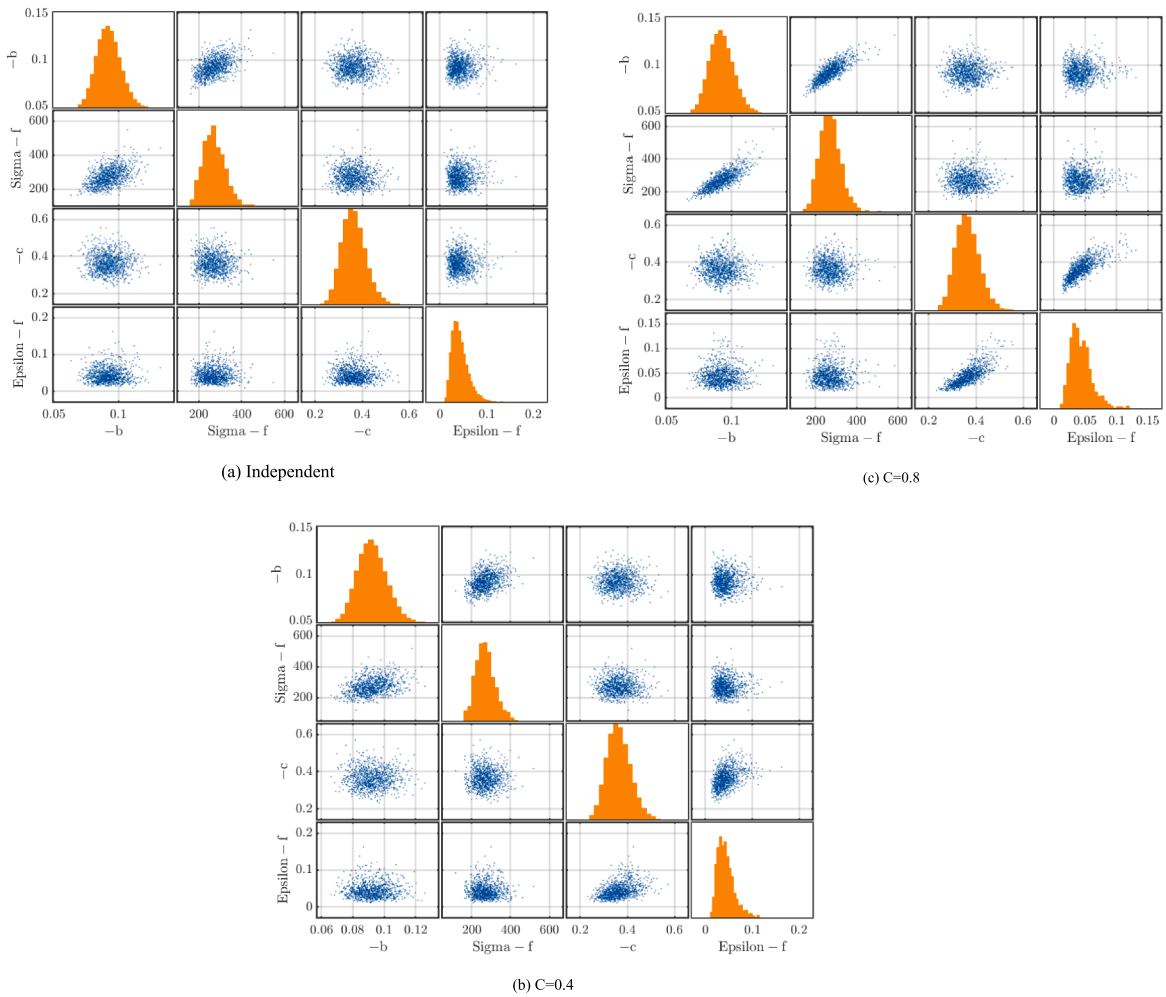


Fig. 4. Correlation Analysis of Material Parameters of WAAM (0°) for the stochastic analysis.

(WAAM-0°). The fatigue cycle of the transition reversals ( $N_T$ ) of structural steel is much less than it of WAAM stainless because of modulus difference.

### 3. Probabilistic fatigue life analysis

With the increasing attention on structural reliability and integrity, probabilistic fatigue models are generally used to consider the multiple uncertainty sources on fatigue lifetime. Zhu et al. [51] proposed a probabilistic framework for fatigue life prediction and reliability assessment of an engine high pressure turbine disc, which provides a valuable reference for engineering structural design and promote the transformation from deterministic to reliability design. Zhu et al. [52] developed and implemented a computational-experimental framework for fatigue reliability assessment of bladed disks, quantified the uncertainty from experimental data, material properties, and loads, which increases the benefit of these methods to extend component lifetimes as well as reliable assessment in structural safety enhancement. So, identification and modelling of fatigue life uncertainty are crucial for the fatigue design quantification. In the stochastic analysis, fatigue life can be predicted by the materials parameters of the CMM equation and a corresponding probability density function (PDF). The above four material parameters, including their dependence structures, can be grouped together as a random vector together with a probability density function (PDF), expressed as  $X \rightarrow f_X(x)$ . The “Lognormal” distribution is used as the cumulative distribution function (CDF), see Eq. (2).

$$F_X(x) = \frac{1}{2} + \frac{1}{2} \operatorname{erf} \left( \frac{\ln x - \lambda}{\sqrt{2} \zeta} \right) \tag{2}$$

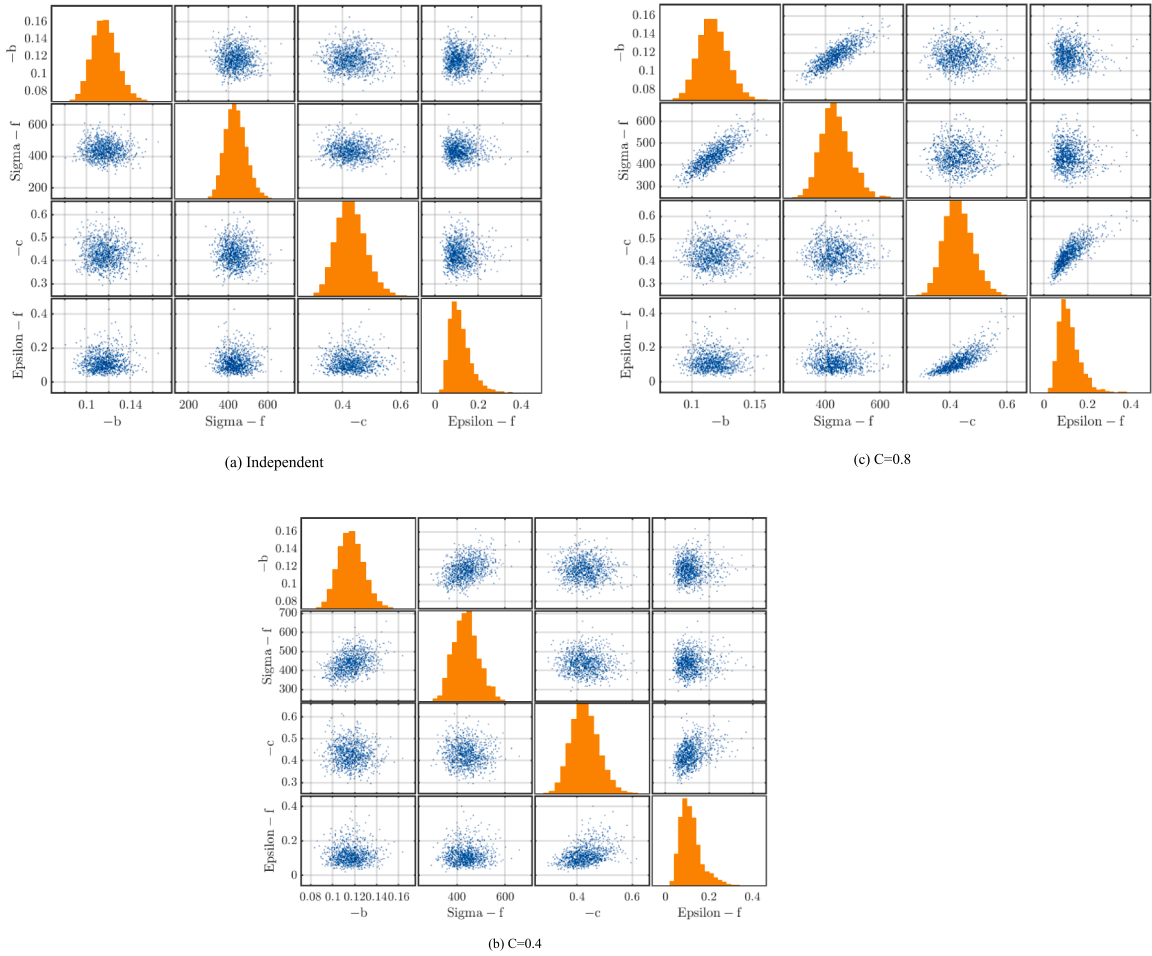


Fig. 5. Correlation Analysis of Material Parameters of WAAM (90°) for the stochastic analysis.

where:  $\lambda$  and  $\zeta$  are the mean value and standard deviation of material parameters. The 4-dimensional CDF is simply specified as a set of 4 univariate distributions  $F_{X_1}, F_{X_2}, F_{X_3}$  and  $F_{X_4}$  defined based on mean values and standard deviation of  $\sigma_f, b, \varepsilon_f,$  and  $c$ , in Table 6. The copula, used to describe the dependence structures of each material parameter, is generally defined as a multivariate distribution over  $[0, 1]^4$ . The multivariate joint distribution is expressed in terms of univariate marginal distribution functions based on Sklar's theorem [53]. The copula  $C$  between the material parameters input vector of CMM equation  $X = \{ X_1 \ X_2 \ X_3 \ X_4 \}$  and marginal  $F_{X_1}, F_{X_2}, F_{X_3}$  and  $F_{X_4}$  can be expressed as follows:

$$F_X(x) = C[F_{X_1}(x_1), F_{X_2}(x_2), F_{X_3}(x_3), F_{X_4}(x_4)] \tag{3}$$

where: the copula  $C$  is the function that links the marginal  $F_{X_i}$  of random vectors to its joint cumulative distribution function (CDF). The copula  $C$  is independent to the marginal  $F_{X_i}$ , only describes the statistical interactions among the components  $X_i$  of input vector  $X$ , and  $C$  is unique for the continuous CDF. The joint CDF of Eq. (2) could be obtained by differentiation:

$$f_X(x) = c(F_{X_1}(x_1), F_{X_2}(x_2), F_{X_3}(x_3), F_{X_4}(x_4)) \prod_{i=1}^M f_{X_i}(x_i) \tag{4}$$

The copula density function  $c(\cdot)$  can be obtained as follows:

$$c(x_1, x_2, x_3, x_4) = \frac{\partial^4 C(x_1, x_2, x_3, x_4)}{\partial x_1 \partial x_2 \partial x_3 \partial x_4} \tag{5}$$

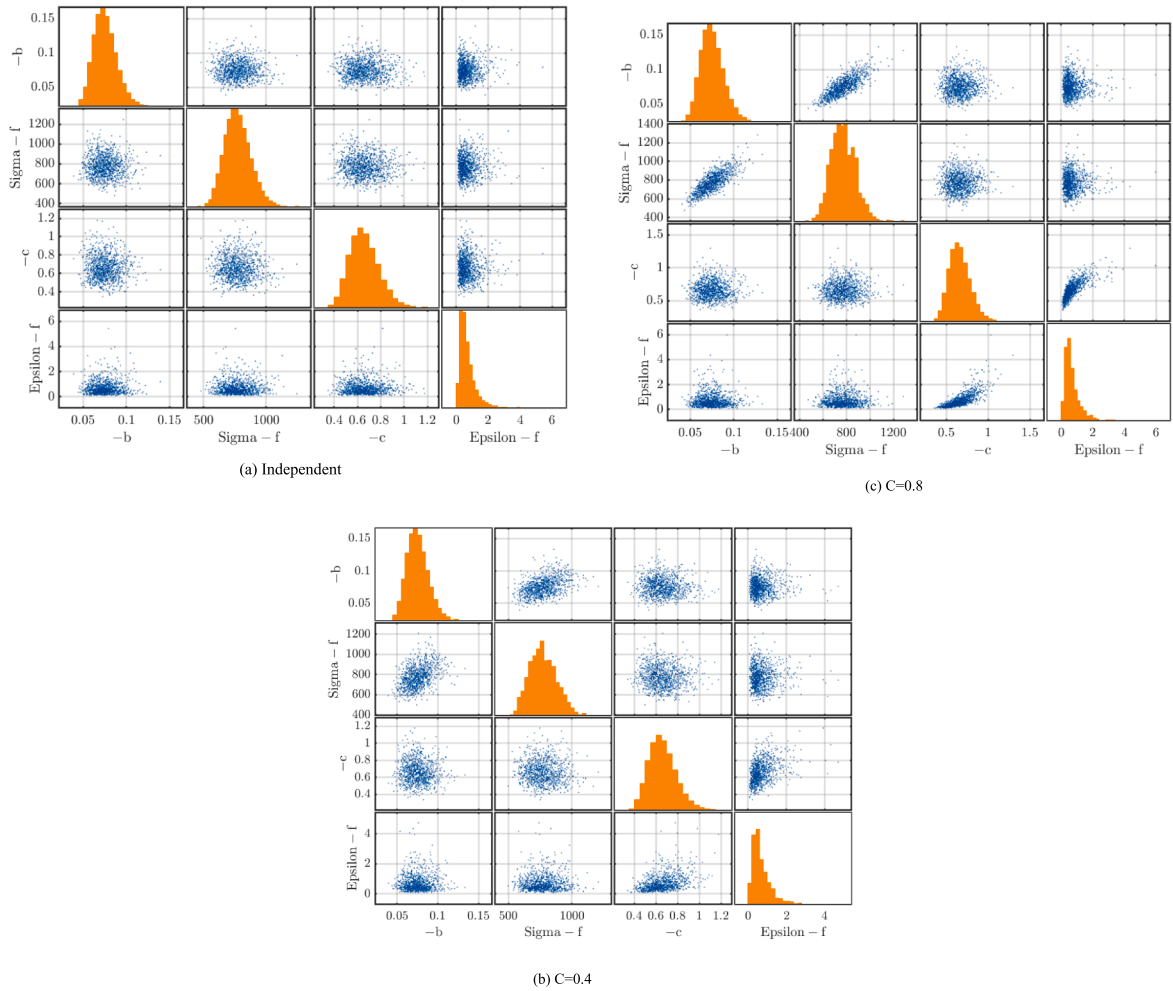


Fig. 6. Correlation Analysis of Material Parameters of S355 for the stochastic analysis.

Based on Bayes' rule, the conditional density could be expressed as follows:

$$f_{X_1|X_2, X_3, X_4}(x_1|x_2, x_3, x_4) = \frac{f_X(x)}{\prod_{i=2}^4 f_{X_i}(x_i)} = c(F_{X_1}(x_1), F_{X_2}(x_2), F_{X_3}(x_3), F_{X_4}(x_4))f_{X_1}(x_1) \tag{6}$$

For independent copula, the copula and joint CDF expression is as follows:

$$C(x_1, x_2, x_3, x_4) = \prod_{i=1}^4 x_i \tag{7}$$

$$F_X(x) = \prod_{i=1}^4 F_{X_i}(x_i) \tag{8}$$

The independent copula density is 1.0.

For Gaussian copula, the copula is expressed as follows:

$$C(x_1, x_2, x_3, x_4, R) = \Phi_4(\Phi^{-1}(x_1), \Phi^{-1}(x_2), \Phi^{-1}(x_3), \Phi^{-1}(x_4); R) \tag{9}$$

where:  $R$  is the linear correlation matrix of the multivariate Gaussian distribution associated with the Gaussian copula,  $\Phi_4(\cdot)$  is the cumulative distribution function of an 4-variate Gaussian distribution with mean 0 and correlation matrix  $R$ ;  $\Phi^{-1}(\cdot)$  is the inverse

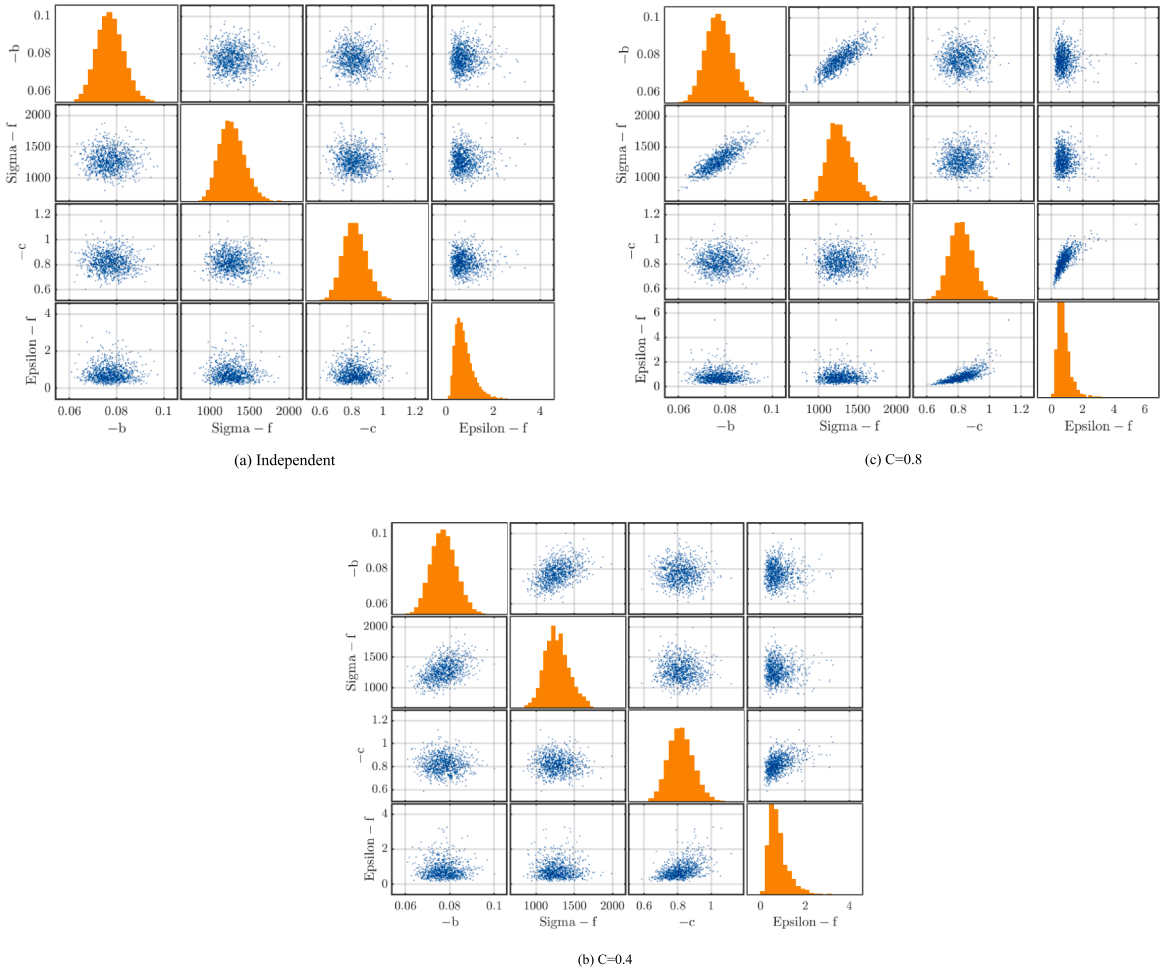


Fig. 7. Correlation Analysis of Material Parameters for the stochastic analysis.

cumulative distribution function of the standard normal distribution.

Meggiolaro and Castro [54] conducted an extensive statistical evaluation of the existing CMM parameter based on 845 fatigue test results, including 724 steels, 81 aluminum alloys, and 15 titanium alloys. The correlations between the fatigue ductility coefficient,  $\epsilon_f$ , and the fatigue strength coefficient is very less. Hence, three different dependence structures of the material parameters of the CMM equation is considered in this paper. The independent copula is used as the first dependence structures among the material parameters, the Gaussian copula with a coefficient 0.4 is used between material parameters  $\sigma_f$  and  $b$ , between  $\epsilon_f$  and  $c$ , respectively, as the second dependence structures among the material parameters, and the Gaussian copula with a coefficient 0.8 is used between material parameters  $\sigma_f$  and  $b$ , between  $\epsilon_f$  and  $c$ , respectively, as the third dependence structures among the material parameters. The correlations analysis of material parameters with different copula strategies is shown in Fig. 4 for WAAM stainless steel along printing direction, in Fig. 5 for WAAM stainless steel vertical to the printing direction, in Fig. 6 for structural steel S355, and in Fig. 7 for structural steel S690, based on [55].

The stochastic analysis of strain-fatigue life relationship is carried out using MATLAB software [56] with the flow chart illustrated in Fig. 8, where the stochastic analysis results in terms of strain-life are given to  $10^0 \leq N \leq 10^8$ . The stochastic analysis results of the strain-fatigue life relationship for WAAM stainless steel and structural steel using independent copula sampling strategies are shown in Fig. 9. The strain-fatigue life relationships with 95%, 97.7%, and 99% guarantee rate are also calculated, shown as a red line in Fig. 9. The parameters of the CMM equation using independent copula with 95%, 97.7%, and 99% guarantee rate are fitted again based on the stochastic analysis results, summarized in Table 7.

The strain amplitude  $\Delta\epsilon_i$  of the  $i^{th}$  material parameter vector, see the flow chart of Fig. 8, is normalized by the average strain

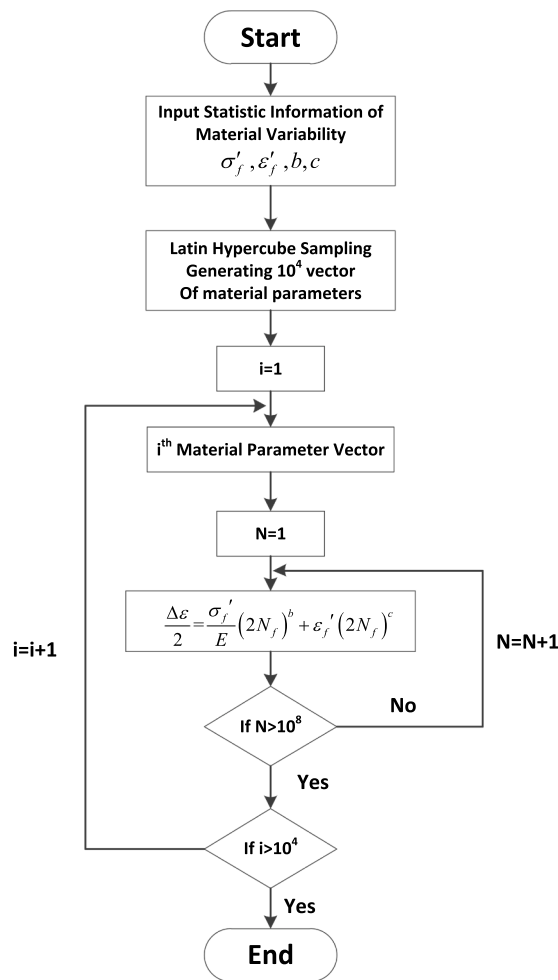


Fig. 8. Flow chart of stochastic analysis of strain-fatigue life relationship.

amplitude  $\Delta\epsilon_m$  during the stochastic analysis. The non-parametric inference [56] was used to fit the strain amplitude ratio ( $\Delta\epsilon_i/\Delta\epsilon_m$ ) distribution at different fatigue cycles from  $1 \times 10^3$  to  $1 \times 10^7$ . The normalized strain amplitude distribution at fatigue cycle  $1 \times 10^3$ ,  $1 \times 10^4$ ,  $1 \times 10^5$ ,  $1 \times 10^6$ , and  $1 \times 10^7$  through stochastic analysis using independent copula sampling strategies is shown in Fig. 10. With the increasing of fatigue cycle, the maximum density of the strain amplitude ratio,  $\Delta\epsilon_i/\Delta\epsilon_m$ , is gradually increased to 1.0. For WAAM stainless steel both parallel and vertical to the printing direction, and structural steel S355, the strain amplitude ratio,  $\Delta\epsilon_i/\Delta\epsilon_m$ , corresponding to maximum probability density, is gradually increased with certain increasing interval from fatigue cycle  $1 \times 10^3$  to fatigue cycle  $1 \times 10^7$ . However, the strain amplitude ratio,  $\Delta\epsilon_i/\Delta\epsilon_m$ , at the maximum probability density at fatigue cycle  $1 \times 10^3$  of structural steel S690 is much smaller than it at other fatigue cycles from  $1 \times 10^4$  to  $1 \times 10^7$ . The strain amplitude ratio,  $\Delta\epsilon_i/\Delta\epsilon_m$ , at the maximum probability density is close to 1.0 for structural steel S690 from fatigue cycle  $1 \times 10^4$  to fatigue cycles  $1 \times 10^7$ .

Fig. 11 presented the strain-fatigue life relationship comparisons between WAAM stainless steel and structural steel with 95%, 97.7%, and 99% guarantee rate, respectively, using independent copula sampling strategies. Due to the larger scattering of structural steel S355, the fatigue performance of WAAM-90° with 95%, 97.7% and 99% guarantee rate exposed to low cycle fatigue loading (from 100 to 20000) is better than the structural steel S355. The fatigue performance vertical to printing direction (WAAM-90°) is also better than it along the printing direction (WAAM-0°) considering the typical guarantee rate. The fatigue cycle of the transition reversals ( $N_T$ ) of structural steel is also much less than it of WAAM stainless after considering different guarantee rates. The fatigue behavior of S355 structural steel shows better performance when compared to WAAM-0° stainless, from low-cycle- (LCF) to high-cycle-fatigue (HCF) regimes, as well as for fatigue regimes above 20,000 cycles when also compared to WAAM-90° stainless.

The stochastic analysis of the strain-fatigue life relationship is also conducted with different copula strategies based on the flow chart illustrated in Fig. 8. The comparison of strain-fatigue life relationship with a 95.5% guarantee rate using different copula

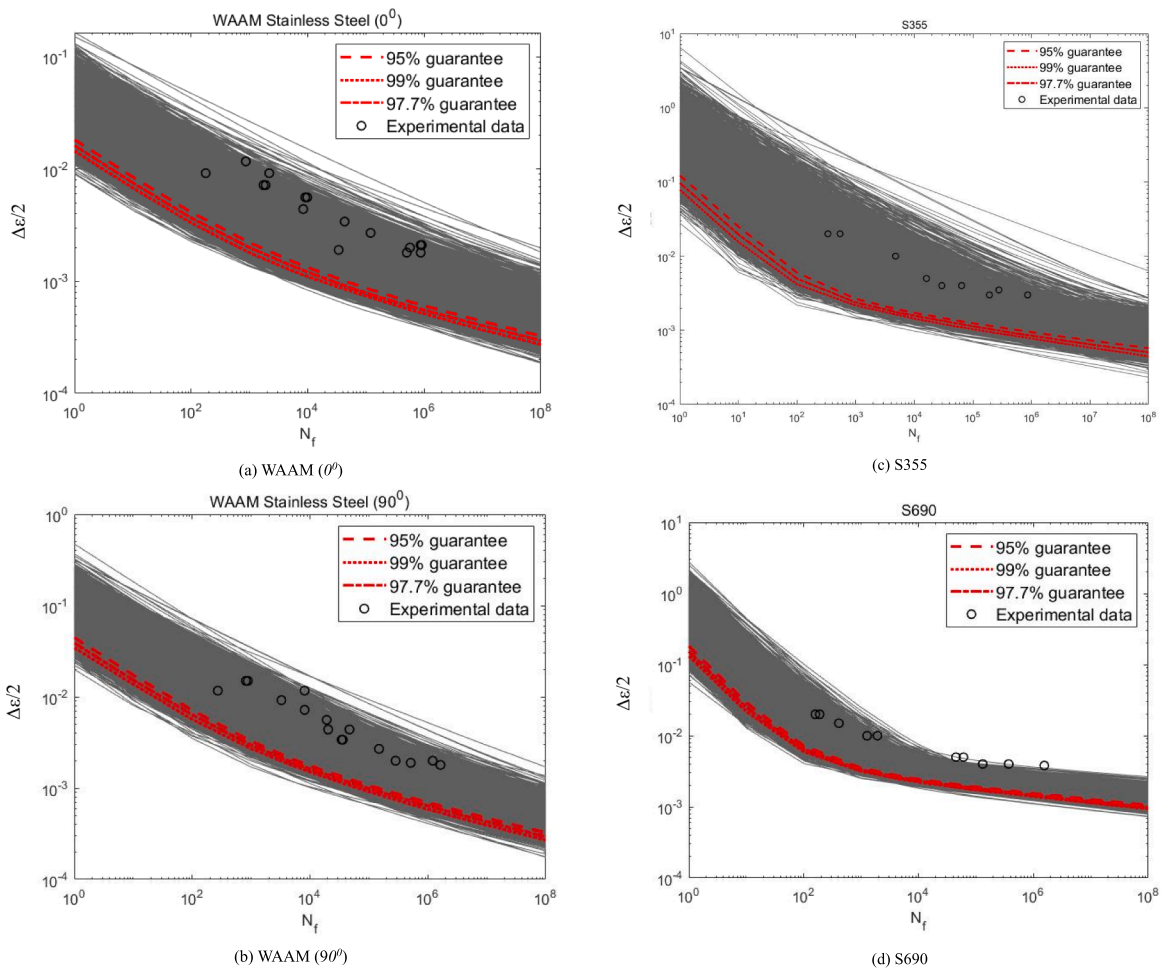


Fig. 9. Stochastic analysis of fatigue life for WAAM and Structural Steel using independent copula.

Table 7  
Fitted parameters of CMM equation using independent copula sampling strategy.

Materials		WAAM		S355	S690
		0°	90°		
95% Guarantee	$\sigma_f^c$	304.7	360.9	914.3	1282.0
	$b$	-0.1162	-0.1233	-0.1105	-0.0949
	$\epsilon_f^c$	0.0216	0.0561	0.1960	0.3170
	$c$	-0.4004	-0.4378	-0.7379	-0.8512
97.7% Guarantee	$\sigma_f^c$	288.0	437.9	900.8	1231.0
	$b$	-0.1171	-0.1384	-0.1164	-0.0953
	$\epsilon_f^c$	0.0188	0.0481	0.1538	0.2687
	$c$	-0.4040	-0.4463	-0.7484	-0.8516
99% Guarantee	$\sigma_f^c$	356.8	444.5	934.0	1240.0
	$b$	-0.1348	-0.1424	-0.1261	-0.0999
	$\epsilon_f^c$	0.0170	0.0420	0.1271	0.2224
	$c$	-0.4452	-0.4551	-0.7795	-0.8493

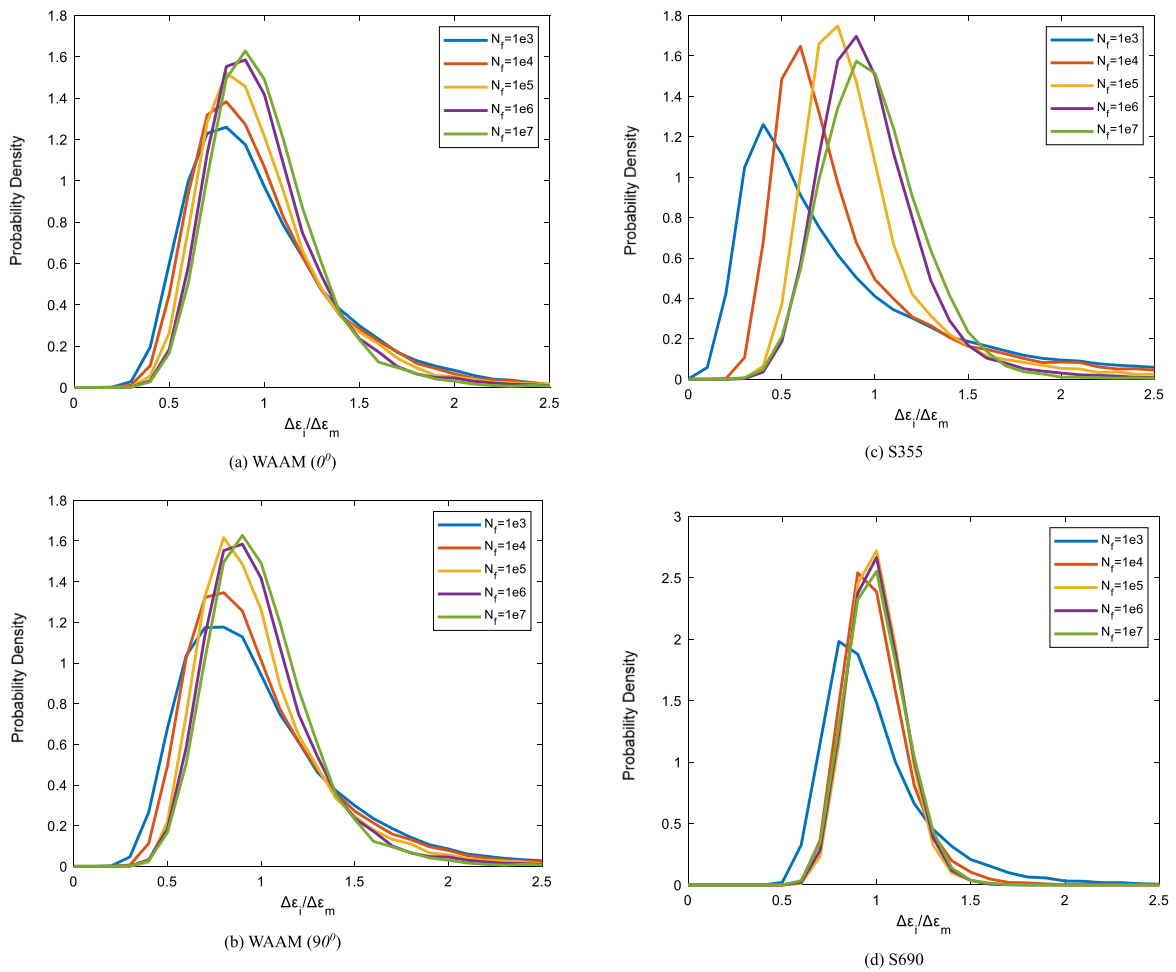


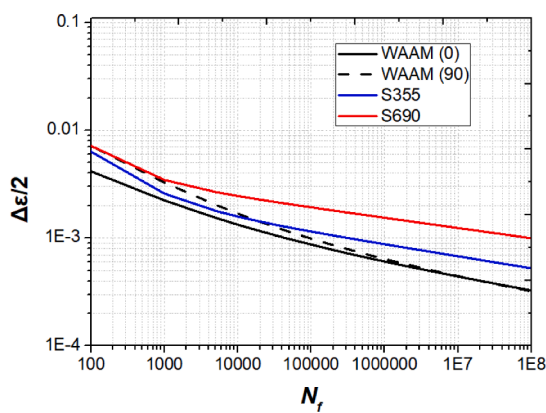
Fig. 10. Normalized Strain Amplitude Distribution at different cycles through stochastic analysis using independent copula.

strategies is shown in Fig. 12. It is noted that 95% (Independent) denoted that the independent copula is used in the Latin hypercube sampling strategies, 95% (0.4) and 95% (0.8) denoted that the Gaussian copula between material parameters  $\sigma_f$  and  $b$ , between  $\epsilon_f$  and  $c$  is used with a coefficient 0.4 and 0.8 respectively. The stochastic analysis results showed that the copula strategy has a large influence on the probabilistic strain-fatigue life relationship. The larger copula coefficient between material parameters  $\sigma_f$  and  $b$ , and between  $\epsilon_f$  and  $c$ , contribute to a good fatigue behavior with a 95.5% guarantee rate. Table 8 lists the fitted parameters of the CMM equation using different copula strategies with a 95% guarantee rate. In Table 9, the fitted parameters of CMM equations with different probability guarantee rate with constant exponent, for the materials under consideration, are presented.

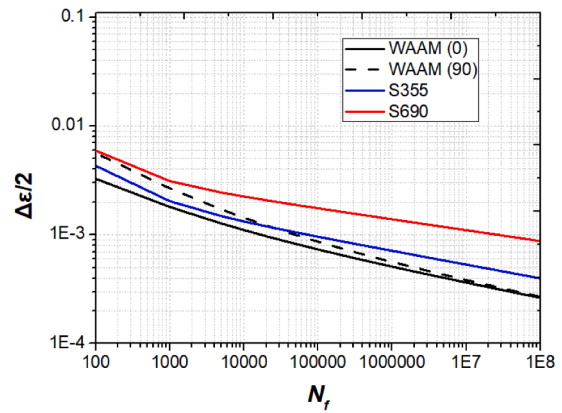
#### 4. Exponent effects on stochastic prediction results

Quantifications of the input variables and their variations and potential interactions is very important to assess the reliability of fatigue behaviors. Meggiolaro and Castro [54] indicated that the combination of constant values for the  $b$  and  $c$  exponents, and reasonable estimations for the fatigue strength coefficient contributes to a good prediction. Hence, it is important to discuss the exponent effects on the probabilistic fatigue life obtained from the stochastic analysis.

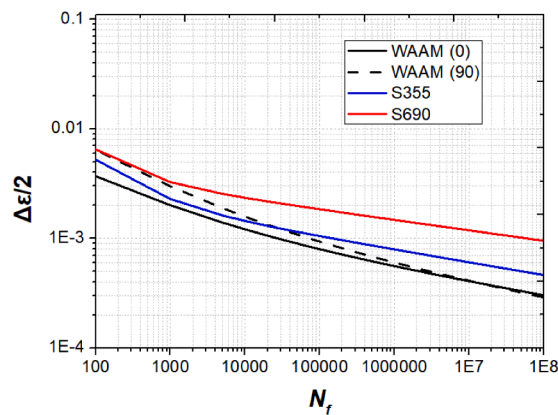
Fig. 13 showed the correlation analysis on material parameters of the WAAM stainless steel which is parallel and vertical to the printing direction with the assumption that exponents  $b$  and  $c$  are constant. The stochastic analysis of the strain-fatigue life relationship is conducted, based on the sampling strategies presented in Fig. 13. The exponent effects on the probabilistic strain-fatigue life relationship of the WAAM stainless steel are illustrated in Fig. 14. The results showed that the probabilistic fatigue behavior of the WAAM stainless steel estimated by the constant exponent sampling strategy is better when compared to the varied exponent sampling strategy. The strain amplitude ration between varied exponent and constant exponent of WAAM stainless steel parallel to printing direction is 0.87 for a 95% guarantee rate, 0.85 for a 97.7% guarantee rate and 0.84 for a 99% guarantee rate at fatigue life cycle  $1 \times 10^3$ , and is 0.88 for a 95% guarantee rate, 0.84 for a 97.7% guarantee rate and 0.83 for a 99% guarantee rate at fatigue life cycle  $1 \times 10^4$ , and is 0.88 for a 95% guarantee rate, 0.86 for a 97.7% guarantee rate and 0.84 for a 99% guarantee rate at fatigue life cycle  $1 \times 10^5$ .



(a) With 95% Guarantee rate



(c) With 99% Guarantee rate



(b) With 97.7% Guarantee rate

Fig. 11. Fatigue life comparisons between WAAM and Structural Steel with different guarantee rate using independent copula.

$10^5$ , and is 0.90 for a 95% guarantee rate, 0.87 for a 97.7% guarantee rate and 0.84 for a 99% guarantee rate at fatigue life cycle  $1 \times 10^6$ . The strain amplitude ration between varied exponent and constant exponent of WAAM stainless steel vertical to printing direction is 0.87 for a 95% guarantee rate, 0.85 for a 97.7% guarantee rate and 0.83 for a 99% guarantee rate at fatigue life cycle  $1 \times 10^3$ , and is 0.86 for a 95% guarantee rate, 0.85 for a 97.7% guarantee rate and 0.82 for a 99% guarantee rate at fatigue life cycle  $1 \times 10^4$ , and is 0.86 for a 95% guarantee rate, 0.84 for a 97.7% guarantee rate and 0.82 for a 99% guarantee rate at fatigue life cycle  $1 \times 10^5$ , and is 0.86 for a 95% guarantee rate, 0.83 for a 97.7% guarantee rate and 0.81 for a 99% guarantee rate at fatigue life cycle  $1 \times 10^6$ .

Fig. 15 showed the correlation analysis on material parameters of structural steel, including S355 and S690, with the assumption that exponents,  $b$  and  $c$ , are constant. The stochastic analysis of the strain-fatigue life relationship is conducted, based on the sampling strategies presented in Fig. 15. The exponent effects on probabilistic strain-fatigue life relationship of structural steel are illustrated in Fig. 16. A similar trend is observed compared with the WAAM stainless steel; the stochastic analysis results also showed that the probabilistic fatigue behavior predicted by the constant exponent sampling strategy is better than it predicted by the varied exponent sampling strategy. The strain amplitude ration between constant exponent and varied exponent of S355 is 0.77 for a 95% guarantee rate, 0.75 for a 97.7% guarantee rate and 0.74 for a 99% guarantee rate at fatigue life cycle  $1 \times 10^3$ , and is 0.85 for a 95% guarantee rate, 0.83 for a 97.7% guarantee rate and 0.82 for a 99% guarantee rate at fatigue life cycle  $1 \times 10^4$ , and is 0.89 for a 95% guarantee rate, 0.85 for a 97.7% guarantee rate and 0.82 for a 99% guarantee rate at fatigue life cycle  $1 \times 10^5$ , and is 0.86 for a 95% guarantee rate, 0.82 for a 97.7% guarantee rate and 0.79 for a 99% guarantee rate at fatigue life cycle  $1 \times 10^6$ .

The strain amplitude ration between constant exponent and varied exponent of S690 is 0.87 for a 95% guarantee rate, 0.84 for a 97.7% guarantee rate and 0.81 for a 99% guarantee rate at fatigue life cycle  $1 \times 10^3$ , and is 0.76 for a 95% guarantee rate, 0.75 for a 97.7% guarantee rate and 0.74 for a 99% guarantee rate at fatigue life cycle  $1 \times 10^4$ , and is 0.68 for a 95% guarantee rate, 0.67 for a

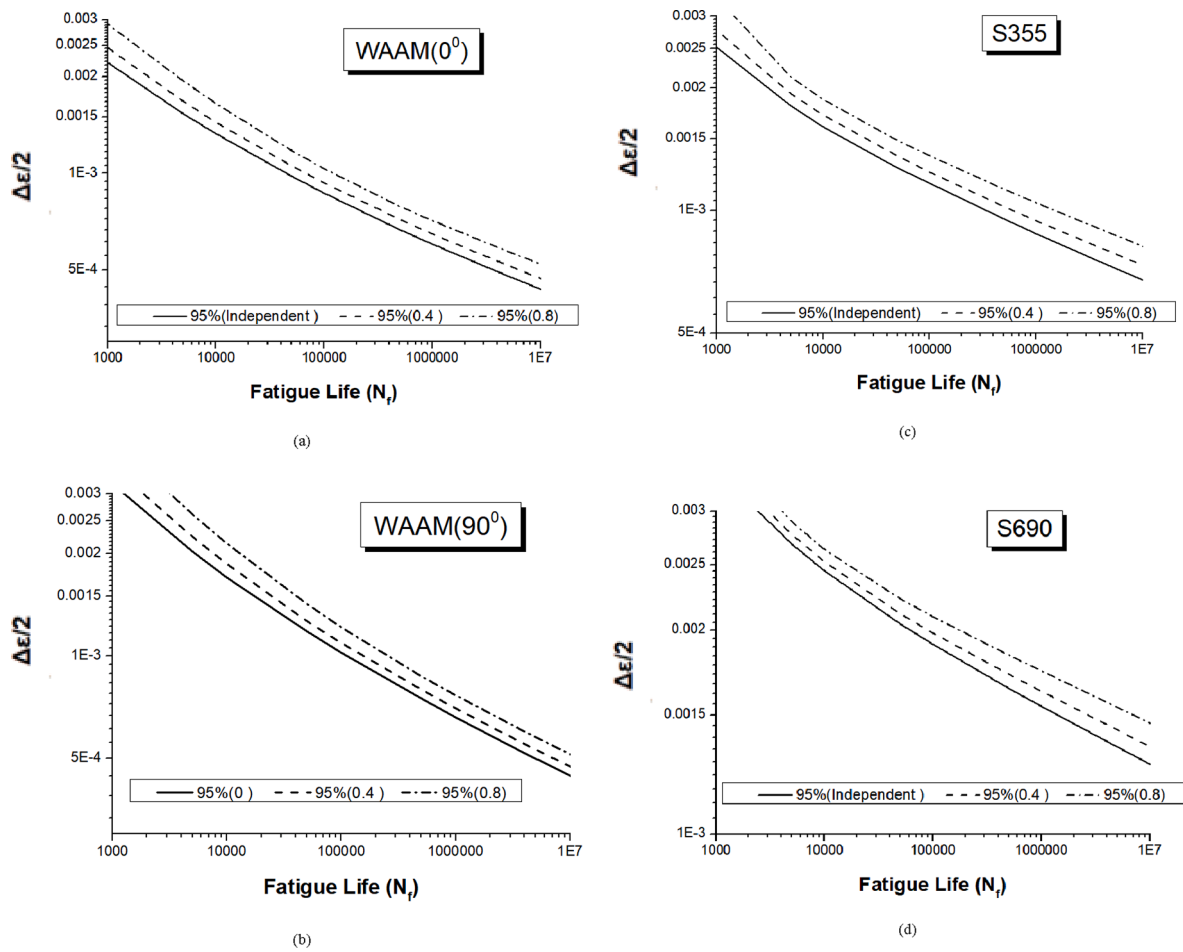


Fig. 12. Fatigue life comparisons with a 95% Guarantee rate using different copula strategies.

**Table 8**  
Copula coefficients effects on fitted parameters of CMM equation with 95% guarantee.

Materials		With 95% Guarantee		
		Independent	C = 0.4	C = 0.8
WAAM ( $0^\circ$ )	$\sigma_f$	304.7	251.6	169.2
	$b$	-0.1162	-0.1036	-0.0870
	$\epsilon_f$	0.0216	0.0224	0.0229
	$c$	-0.4004	-0.3688	-0.3164
WAAM ( $90^\circ$ )	$\sigma_f$	360.9	263.2	62.3
	$b$	-0.1233	-0.1027	-0.0250
	$\epsilon_f$	0.0561	0.0571	0.0581
	$c$	-0.4378	-0.4083	-0.3354
S355	$\sigma_f$	914.3	662.6	202.3
	$b$	-0.1105	-0.0859	-0.0104
	$\epsilon_f$	0.1960	0.1950	0.198
	$c$	-0.7379	-0.6449	-0.5337
S690	$\sigma_f$	1282.0	1465.0	1541.0
	$b$	-0.0949	-0.0913	-0.0904
	$\epsilon_f$	0.3170	0.0534	0.0594
	$c$	-0.8512	-0.9965	-0.8993

**Table 9**

Fitted parameters of CMM equation with different probability guarantee rate with constant exponent.

Materials		WAAM		S355	S690
		0°	90°		
95% Guarantee	$\sigma_f$	441.5	512.3	912.1	1393.0
	$b$	-0.1354	-0.1337	-0.0995	-0.0892
	$\varepsilon_f$	0.0191	0.0542	0.1877	0.0483
	$c$	-0.3840	-0.4326	-0.6631	-0.9344
97.7% Guarantee	$\sigma_f$	345.0	498.7	939.8	1344.0
	$b$	-0.1231	-0.1341	-0.1041	-0.0898
	$\varepsilon_f$	0.0171	0.0469	0.1485	0.0408
	$c$	-0.3712	-0.4311	-0.6670	-0.9480
99% Guarantee	$\sigma_f$	243.8	545.3	900.5	1296.0
	$b$	-0.1075	-0.1412	-0.1042	-0.0900
	$\varepsilon_f$	0.0155	0.0404	0.1187	0.0341
	$c$	-0.3475	-0.4366	-0.6642	-0.9380

97.7% guarantee rate and 0.67 for a 99% guarantee rate at fatigue life cycle  $1 \times 10^5$ , and is 0.63 for a 95%, 97.7% and 99% guarantee rate at fatigue life cycle  $1 \times 10^6$ .

## 5. Summary and conclusions

In this paper, Coffin-Manson and Morrow's (CMM) Fatigue Law is employed to describe the fatigue life of WAAM stainless steel, structural steels S355 and S690, in the literature. The following conclusions are drawn:

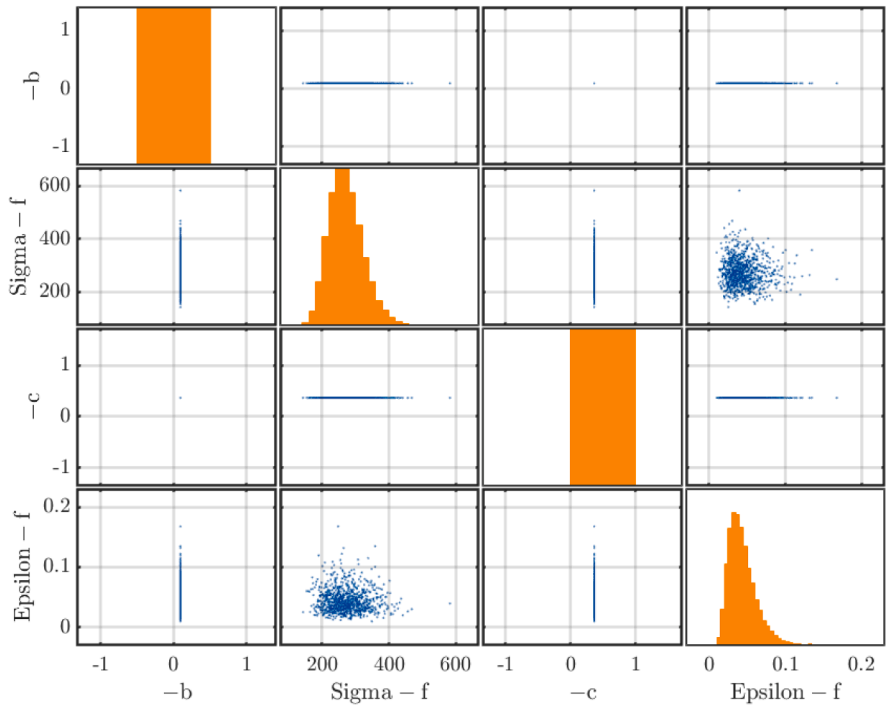
- (1) The fatigue performance of structural steel is better than the WAAM stainless steel, the fatigue performance vertical to printing direction (WAAM-90°) is better than it along the printing direction (WAAM-0°), the fatigue cycle of the transition reversals of structural steel is much less than it of WAAM stainless.
- (2) The parameters with 95%, 97.7%, and 99% guarantee rates of CMM Fatigue Law is obtained by a stochastic analysis using Latin hypercube sampling strategies. The non-parametric inference was used to investigate the strain amplitude ratio  $\Delta\varepsilon_i/\Delta\varepsilon_m$  distribution at different fatigue cycles from  $1 \times 10^3$  to  $1 \times 10^7$ . With the increasing the fatigue cycle, the maximum density of the strain amplitude ratio  $\Delta\varepsilon_i/\Delta\varepsilon_m$  is gradually increased to 1.0. The stochastic analysis results showed that the copula strategy has a large influence on the probabilistic strain-fatigue life relationship. The larger copula coefficient between material parameters,  $\sigma_f$  and  $b$ , and, between  $\varepsilon_f$  and  $c$ , contribute to a good fatigue behavior with a 95.5% guarantee rate.
- (3) The exponent effects on the probabilistic fatigue life are investigated by comparing the stochastic analysis results using a constant exponent sampling strategy and varied constant sampling strategy. The results showed that the probabilistic fatigue behavior of both WAAM stainless steel and structural steel predicted by the constant exponent sampling strategy is better than it predicted by the varied exponent sampling strategy.

## CRedit authorship contribution statement

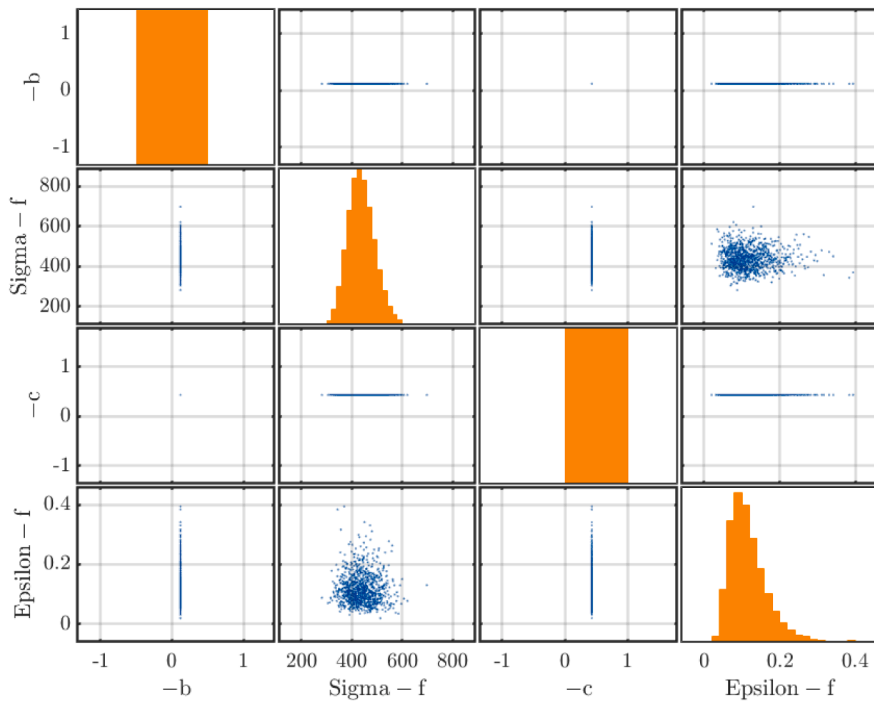
**Haohui Xin:** Investigation, Formal analysis, Methodology, Validation, Writing - original draft. **José A.F.O. Correia:** Investigation, Formal analysis, Methodology, Validation, Writing - original draft. **Milan Veljkovic:** Validation, Supervision, Writing - review & editing. **Youyou Zhang:** Investigation, Formal analysis, Validation, Writing - review & editing. **Filippo Berto:** Validation, Writing - review & editing. **Abílio M.P. de Jesus:** Validation, Writing - review & editing.

## Declaration of Competing Interest

The authors declare that they have no known competing financial interests or personal relationships that could have appeared to influence the work reported in this paper.

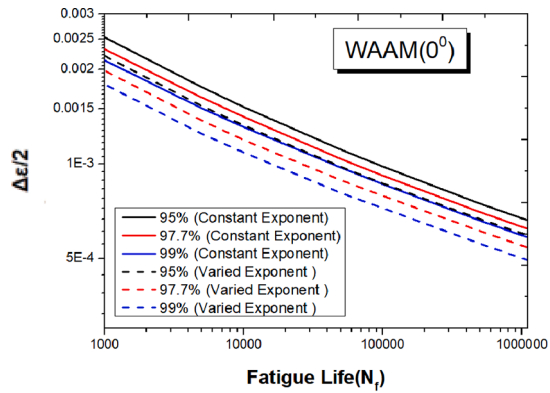


(a) WAAM (0°)

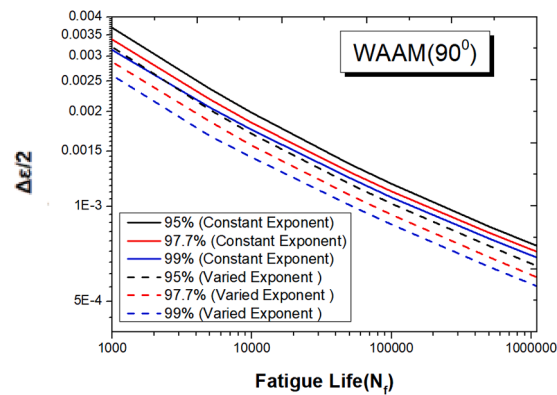


(b) WAAM (90°)

Fig. 13. Correlation Analysis of Material Parameters of WAAM with constant exponent.



(a)



(b)

**Fig. 14.** Exponent effects on fatigue life of WAAM stainless steel with different Guarantee rate.

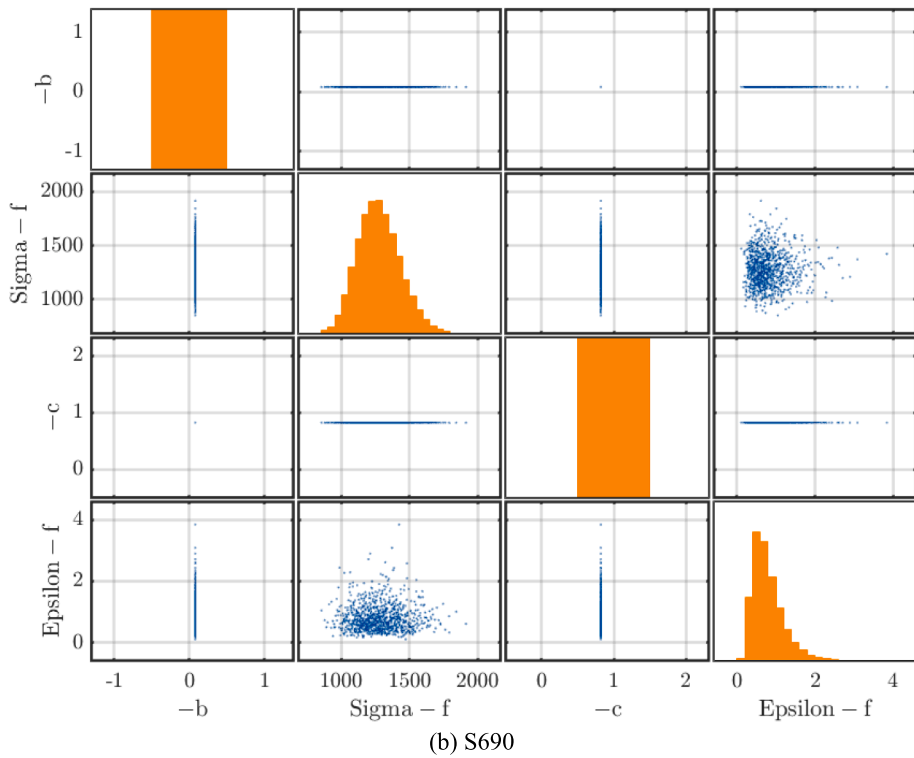
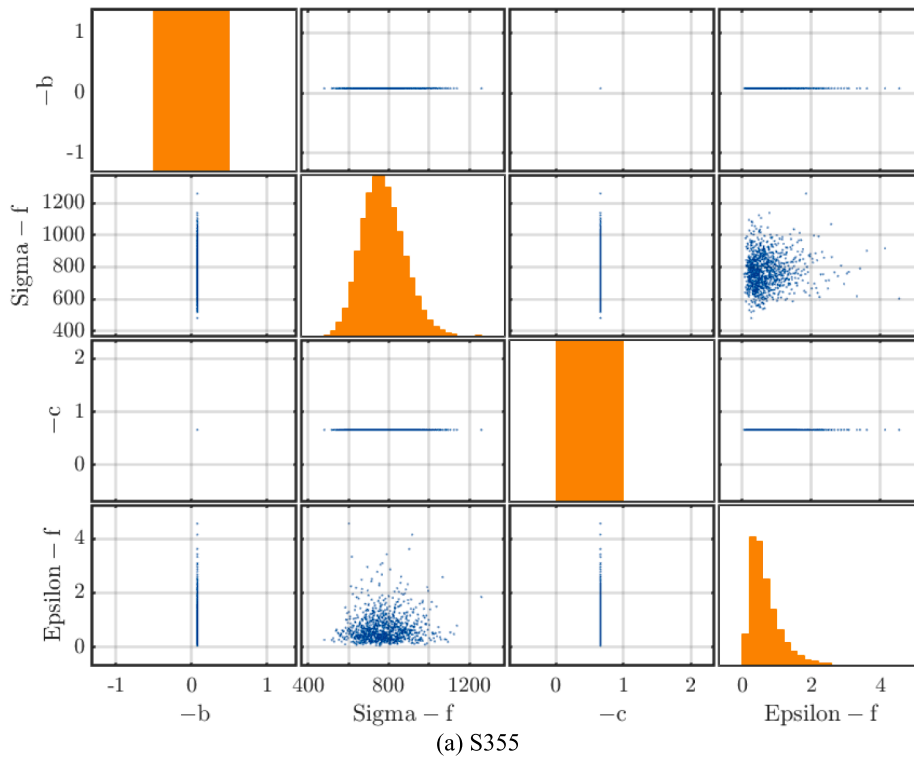


Fig. 15. Correlation Analysis of Material Parameters of structural steel with constant exponent.

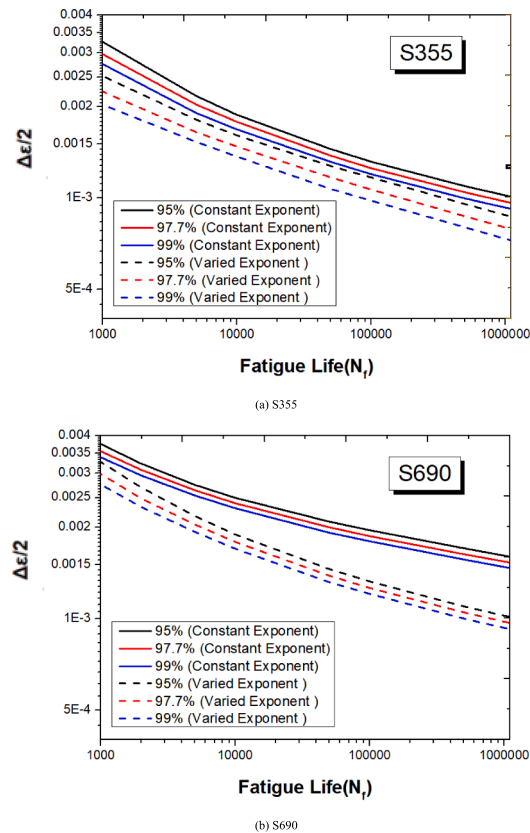


Fig. 16. Exponent effects on fatigue life of structural steel with different Guarantee rate.

## Acknowledgments

Thanks to P.A. de Vries at Steel & Composite Structures Section of the Delft University of Technology (TUDelft) providing the documents related to fatigue tests of the WAAM stainless steel. This research was also supported by the National Natural Science Foundation (Grants #51808398) of the People's Republic of China, base funding - UIDB/04708/2020 and programmatic funding - UIDP/04708/2020 of the CONSTRUCT - Instituto de I&D em Estruturas e Construções - FCT/MCTES (PIDDAC), High-Strength Steels in Metalomechanics 4.0 (POCI-01-0247-FEDER-068492) by P2020|COMPETE funds, and project grant (UTA-EXPL/IET/0111/2019) SOS-WindEnergy - Sustainable Reuse of Decommissioned Offshore Jacket Platforms for Offshore Wind Energy by national funds (PIDDAC) through the Portuguese Science Foundation (FCT/MCTES).

## References

- [1] C. Buchanan, L. Gardner, Metal 3D printing in construction: a review of methods, research, applications, opportunities and challenges, *Eng. Struct.* 180 (2019) 332–348.
- [2] A. Paolini, S. Kollmannsberger, E. Rank, Additive manufacturing in construction: a review on processes, applications, and digital planning methods, *Addit. Manuf.* 30 (2019) 100894.
- [3] H. Xin, W. Sun, J. Fish, A surrogate modeling approach for additive-manufactured materials, *Int. J. Multiscale Comput. Eng.* 15 (2017) 525–543, <https://doi.org/10.1615/IntJMCompEng.2017024632>.
- [4] H. Xin, W.C. Sun, J. Fish, Discrete element simulations of powder-bed sintering-based additive manufacturing, *Int. J. Mech. Sci.* 149 (2018) 373–392.
- [5] T.A. Rodrigues, V. Duarte, R.M. Miranda, T.G. Santos, J.P. Oliveira, Current status and perspectives on wire and arc additive manufacturing (WAAM), *Materials (Basel)* 12 (2019) 1121.
- [6] C.R. Cunningham, J.M. Flynn, A. Shokrani, V. Dhokia, S.T. Newman, Invited review article: strategies and processes for high quality wire arc additive manufacturing, *Addit. Manuf.* 22 (2018) 672–686.
- [7] B. Wu, Z. Pan, D. Ding, D. Cuiuri, H. Li, J. Xu, et al., A review of the wire arc additive manufacturing of metals: properties, defects and quality improvement, *J. Manuf. Process* 35 (2018) 127–139.
- [8] H. Xin, M. Veljkovic, Fatigue crack initiation prediction using phantom nodes-based extended finite element method for S355 and S690 steel grades, *Eng. Fract. Mech.* 214 (2019) 164–176.
- [9] H. Xin, M. Veljkovic, Residual stress effects on fatigue crack growth rate of mild steel S355 exposed to air and seawater environments, *Mater. Des.* 108732 (2020).
- [10] H. Xin, J.A.F.O. Correia, M. Veljković, Three-dimensional fatigue crack propagation simulation using extended finite element methods for steel Grades S355 and S690 considering mean stress effects, *Eng. Struct.* 227 (2021) 111414.
- [11] H. Xin, J.A.F.O. Correia, M. Veljkovic, F. Berto, L. Manuel, Residual stress effects on fatigue life prediction using hardness measurements for butt-welded joints made of high strength steels, *Int. J. Fatigue* 106175 (2021).

- [12] J.V. Gordon, C.V. Haden, H.F. Nied, R.P. Vinci, D.G. Harlow, Fatigue crack growth anisotropy, texture and residual stress in austenitic steel made by wire and arc additive manufacturing, *Mater. Sci. Eng. A* 724 (2018) 431–438.
- [13] J. Gordon, J. Hochhalter, C. Haden, D.G. Harlow, Enhancement in fatigue performance of metastable austenitic stainless steel through directed energy deposition additive manufacturing, *Mater. Des.* 168 (2019) 107630.
- [14] M. Wächter, M. Leicher, M. Hupka, C. Leistner, L. Masendorf, K. Treutler, et al., Monotonic and fatigue properties of steel material manufactured by wire arc additive manufacturing, *Appl. Sci.* 10 (2020) 5238.
- [15] R. Biswal, X. Zhang, A.K. Syed, M. Awd, J. Ding, F. Walther, et al., Criticality of porosity defects on the fatigue performance of wire+ arc additive manufactured titanium alloy, *Int. J. Fatigue* 122 (2019) 208–217.
- [16] A. Ermakova, A. Mehmanparast, S. Ganguly, J. Razavi, F. Berto, Investigation of mechanical and fracture properties of wire and arc additively manufactured low carbon steel components, *Theor. Appl. Fract. Mech.* 109 (2020) 102685.
- [17] Argumedo J. Galan, Fatigue behavior and mechanical characterization of austenitic stainless-steel components produced through Wire+, Arc Additive Manufacturing (2020) <http://resolver.tudelft.nl/uuid:c9313a80-39d0-4f00>.
- [18] S. Anderson Goehrke, 3D printed steel pedestrian bridge will soon span an Amsterdam canal. 3D Print, 2015.
- [19] L. Gardner, P. Kyvelou, G. Herbert, C. Buchanan, Testing and initial verification of the world's first metal 3D printed bridge, *J. Constr. Steel Res.* 172 (2020) 106233.
- [20] T. Feucht, J. Lange, B. Waldschmitt, A.-K. Schudlich, M. Klein, M. Oechsner, Welding Process for the Additive Manufacturing of Cantilevered Components with the WAAM. *Adv. Join. Process*, Springer, 2020, pp. 67–78.
- [21] J. Lange, T. Feucht, M. Erven, 3D printing with steel: additive Manufacturing for connections and structures, *Steel Constr.* 13 (2020) 144–153.
- [22] P. Raposo, J.A.F. de O. Correia, A.M.P. De Jesus, R.A.B. Calçada, G. Lesiuk, M. Hebdon, et al., Probabilistic fatigue SN curves derivation for notched components, *Frat Ed Integrita Strutt* 11 (2017).
- [23] J.A.F.O. Correia, A.M.P. De Jesus, A. Fernández-Canteli, Local unified probabilistic model for fatigue crack initiation and propagation: application to a notched geometry, *Eng. Struct.* 52 (2013) 394–407.
- [24] J. Correia, P.J. Huffman, A.M.P. De Jesus, G. Lesiuk, J.M. Castro, R.A.B. Calçada, et al., Probabilistic fatigue crack initiation and propagation fields using the strain energy density, *Strength Mater.* 50 (2018) 620–635.
- [25] J.A.F. de O. Correia, P.J. Huffman, A.M.P. De Jesus, S. Cicero, A. Fernández-Canteli, F. Berto, et al., Unified two-stage fatigue methodology based on a probabilistic damage model applied to structural details, *Theor. Appl. Fract. Mech.* 92 (2017) 252–65.
- [26] A.M.P. De Jesus, H. Pinto, A. Fernández-Canteli, E. Castillo, J.A.F.O. Correia, Fatigue assessment of a riveted shear splice based on a probabilistic model, *Int. J. Fatigue* 32 (2010) 453–462.
- [27] B. Pedrosa, C. Rebelo, H. Gervásio, L.S. da Silva, J.A. Correia, Fatigue of preloaded bolted connections with injection bolts, *Struct. Eng. Int.* 30 (2020) 102–108.
- [28] B. Pedrosa, J.A.F.O. Correia, C. Rebelo, G. Lesiuk, A.M.P. De Jesus, A.A. Fernandes, et al., Fatigue resistance curves for single and double shear riveted joints from old portuguese metallic bridges, *Eng. Fail. Anal.* 96 (2019) 255–273.
- [29] J.A.F. de Oliveira Correia, B.A.S. Pedrosa, P.C. Raposo, A.M.P. De Jesus, H.M. dos Santos Gervásio, G.S. Lesiuk, et al., Fatigue strength evaluation of resin-injected bolted connections using statistical analysis, *Engineering* (2017).
- [30] J.F. Barbosa, R. Carlos Silverio Freire Júnior, J.A.F.O. Correia, A.M.P. De Jesus, R.A.B. Calçada, Analysis of the fatigue life estimators of the materials using small samples, *J. Strain Anal. Eng. Des.* 53 (2018) 699–710.
- [31] B. Pedrosa, J.A.F.O. Correia, C.A.S. Rebelo, M. Veljkovic, Reliability of fatigue strength curves for riveted connections using normal and Weibull distribution functions, *ASCE-ASME J. Risk Uncertain Eng. Syst. Part A Civ. Eng.* 6 (2020) 4020034.
- [32] P.D. Toasa Caiza, T. Ummenhofer, J.A.F.O. Correia, A. De Jesus, Applying the Weibull and Stüssi methods that derive reliable Wöhler curves to historical German bridges, *Pract. Period Struct. Des. Constr.* 25 (2020) 4020029.
- [33] J. Correia, N. Apetre, A. Arcari, A. De Jesus, M. Muñoz-Calvente, R. Calçada, et al., Generalized probabilistic model allowing for various fatigue damage variables, *Int. J. Fatigue* 100 (2017) 187–194.
- [34] J.F. Barbosa, J.A.F.O. Correia, R.C.S. Freire Junior, S.-P. Zhu, A.M.P. De Jesus, Probabilistic SN fields based on statistical distributions applied to metallic and composite materials: State of the art, *Adv. Mech. Eng.* 11 (2019) 1687814019870395.
- [35] A. Mourão, J.A.F.O. Correia, B.V. Ávila, C.C. de Oliveira, T. Ferradosa, H. Carvalho, et al., A fatigue damage evaluation using local damage parameters for an offshore structure. *Proc. Inst. Civ. Eng. Eng. Thomas Telford Ltd*, 2020, pp. 1–35.
- [36] S.-P. Zhu, J.-C. He, D. Liao, Q. Wang, Y. Liu, The effect of notch size on critical distance and fatigue life predictions, *Mater. Des.* 109095 (2020).
- [37] M. Kumar, I.V. Singh, B.K. Mishra, Fatigue crack growth simulations of plastically graded materials using XFEM and J-integral decomposition approach, *Eng. Fract. Mech.* 216 (2019) 106470.
- [38] G. Lesiuk, M. Smolnicki, R. Mech, A. Zięty, C. Fragassa, Analysis of fatigue crack growth under mixed mode (I+ II) loading conditions in rail steel using CTS specimen, *Eng. Fail. Anal.* 109 (2020) 104354.
- [39] J.A.F. de O. Correia, S. Blason, A.M.P. De Jesus, A.F. Canteli, P. Moreira, P.J. Tavares, Fatigue life prediction based on an equivalent initial flaw size approach and a new normalized fatigue crack growth model, *Eng. Fail. Anal.* 69 (2016) 15–28.
- [40] G. Lesiuk, Application of a new, energy-based  $\Delta S^*$  crack driving force for fatigue crack growth rate description, *Materials (Basel)* 12 (2019) 518.
- [41] G. Lesiuk, M. Szata, J.A.F.O. Correia, A.M.P. De Jesus, F. Berto, Kinetics of fatigue crack growth and crack closure effect in long term operating steel manufactured at the turn of the 19th and 20th centuries, *Eng. Fract. Mech.* 185 (2017) 160–174.
- [42] J. Correia, H. Carvalho, G. Lesiuk, A. Mourão, L.F. Grilo, A. de Jesus, et al., Fatigue crack growth modelling of Fão Bridge puddle iron under variable amplitude loading, *Int. J. Fatigue* 136 (2020) 105588.
- [43] J. Correia, A.M.P. De Jesus, A. Fernández-Canteli, R. Brighenti, P. Moreira, R. Calçada, A procedure to obtain the probabilistic kitagawa-takahashi diagram, *UPB Sci. Bull. Ser. Mech. Eng.* 78 (2016) 3–12.
- [44] J. Correia, A.M.P. De Jesus, R. Calçada, B. Pedrosa, C. Rebelo, L.S. da Silva, et al., Statistical analysis of fatigue crack propagation data of materials from ancient portuguese metallic bridges, *Frat Ed Integrita Strutt* 11 (2017) 136–146.
- [45] J. Morrow, Cyclic plastic strain energy and fatigue of metals. *Intern. Frict. damping, Cycl. Plast.*, ASTM International, 1965.
- [46] S.S. Manson, Behavior of materials under conditions of thermal stress, National Advisory Committee for Aeronautics 2933 (1953).
- [47] L.F. Coffin Jr, A study of the effects of cyclic thermal stresses on a ductile metal, *Trans. Am. Soc. Mech. Eng. New York* 76 (1954) 931–950.
- [48] A.M.P. De Jesus, R. Matos, B.F.C. Fontoura, C. Rebelo, L. Simões Da Silva, M. Veljkovic, A comparison of the fatigue behavior between S355 and S690 steel grades, *J. Constr. Steel Res.* 79 (2012) 140–150, <https://doi.org/10.1016/j.jcsr.2012.07.021>.
- [49] W.K. Loh, A.D. Crocombe, M.M.A. Wahab, I.A. Ashcroft, Modelling anomalous moisture uptake, swelling and thermal characteristics of a rubber toughened epoxy adhesive, *Int. J. Adhes. Adhes.* 25 (2005) 1–12.
- [50] EN BS. 10025: Hot rolled products of structural steels. BS EN, 2004, 10025.
- [51] S.-P. Zhu, Q. Liu, Q. Lei, Q. Wang, Probabilistic fatigue life prediction and reliability assessment of a high pressure turbine disc considering load variations, *Int. J. Damage Mech.* 27 (2018) 1569–1588.
- [52] S.-P. Zhu, Q. Liu, W. Peng, X.-C. Zhang, Computational-experimental approaches for fatigue reliability assessment of turbine bladed disks, *Int. J. Mech. Sci.* 142 (2018) 502–517.
- [53] C. Lataniotis, S. Marelli, B. Sudret, UQLab user manual–The Input module. Chair Risk, Saf Uncertain Quantif ETH Zurich, Zurich, Switzerland, Rep No UQLab-V1 (2015) 2–102.
- [54] M.A. Meggiolaro, J.T.P. Castro, Statistical evaluation of strain-life fatigue crack initiation predictions, *Int. J. Fatigue* 26 (2004) 463–476.
- [55] S. Marelli, B. Sudret, UQLab: a framework for uncertainty quantification in Matlab. Vulnerability, uncertainty, risk Quantif. mitigation, *Manag.* (2014) 2554–2563.
- [56] H. Klee, R. Allen, Simulation of dynamic systems with MATLAB® and Simulink®, Crc Press, 2018.